Drop Impact on Superheated Surfaces

Tuan Tran,[1,*] Hendrik J. J. Staat,[1] Andrea Prosperetti,[1,2] Chao Sun,[1,†] and Detlef Lohse[1,‡]

[1]*Physics of Fluids, University of Twente, P.O. Box 217, 7500 AE Enschede, The Netherlands*

[2]*Department of Mechanical Engineering, Johns Hopkins University, Baltimore, Maryland 21218, USA*

(Received 1 November 2011; published 20 January 2012)

At the impact of a liquid droplet on a smooth surface heated above the liquid's boiling point, the droplet either immediately boils when it contacts the surface (''contact boiling''), or without any surface contact forms a Leidenfrost vapor layer towards the hot surface and bounces back (''gentle film boiling''), or both forms the Leidenfrost layer and ejects tiny droplets upward (''spraying film boiling''). We experimentally determine conditions under which impact behaviors in each regime can be realized. We show that the dimensionless maximum spreading γ of impacting droplets on the heated surfaces in both gentle and spraying film boiling regimes shows a universal scaling with the Weber number We ($\gamma \sim \mathrm{We}^{2/5}$), which is much steeper than for the impact on nonheated (hydrophilic or hydrophobic) surfaces ($\gamma \sim \mathrm{We}^{1/4}$). We also interferometrically measure the vapor thickness under the droplet.

DOI: 10.1103/PhysRevLett.108.036101 PACS numbers: 68.08.Bc, 44.35.+c, 47.20.Ma

When a drop impinges gently on a surface heated well above the liquid's boiling temperature, the liquid may evaporate so fast that the drop floats on its own vapor. The vapor layer then acts as a thermally insulating film causing the drop to evaporate much more slowly than if it remained in contact with the surface. This phenomenon is known as the Leidenfrost effect [1]; the temperature at which the evaporation time of the drop reaches its maximum is called the Leidenfrost temperature. Since it was first reported in 1756, various aspects of the Leidenfrost effect have been studied, most importantly the determination of the Leidenfrost temperature for different liquids and surfaces [2,3]. In general, measurements of the Leidenfrost temperature were performed with zero or at most small incident velocity because the characteristic time scale of the impact, of order of several milliseconds, is negligible compared to the drop's total evaporation time. In other words, the Leidenfrost temperature is assumed not to be affected by the impact dynamics (hence to be referred to herein as the static Leidenfrost temperature), and is commonly considered as the lowest boundary of the film boiling regime [4–7]. However, in most realistic situations where the impact velocity is not negligible, the Leidenfrost temperature should be regarded as a dynamic quantity [3] (see review articles [8,9]). One can define the dynamic Leidenfrost temperature T_L as the minimum temperature of the surface at which the developing vapor layer causes an impinging droplet to bounce. As compared to the static case, there have been very few studies that focus on the dependence of T_L on impact conditions. The goal of this Letter is to experimentally determine this dependence and to study droplet impact dynamics on heated surfaces.

For this purpose, we generate droplets by pushing liquid from a syringe at a small rate (≈ 0.05 ml/min) through a pipe and into a capillary needle (inner diameter 0.1 mm). The droplet formed at the needle's tip detaches as soon as the gravitational force overcomes the surface tension. We use two different liquids: milli-Q water (density $\rho_w = 998\ \mathrm{kg/m^3}$, surface tension $\sigma_w = 72 \times 10^{-3}\ \mathrm{N/m}$, viscosity $\nu_w = 10^{-6}\ \mathrm{m^2/s}$), and a Fluorinert liquid FC-72 ($\rho_{\mathrm{fc}} = 1680\ \mathrm{kg/m^3}$, $\sigma_{\mathrm{fc}} = 11.9 \times 10^{-3}\ \mathrm{N/m}$, $\nu_{\mathrm{fc}} = 0.38 \times 10^{-6}\ \mathrm{m^2/s}$, boiling temperature 56 °C). By varying the needle's height, we control the velocity V of the droplet before impacting the surface. We simultaneously capture side-view and bottom-view images of the droplet as it spreads using two synchronous high-speed cameras (Photron Fastcam SA1 & SA2). From the series of recorded images in each experiment, we obtain the impact velocity V, the drop diameter D_0 (typically 1.7 and 2.2 mm for water and 1.1 mm for FC-72), and the maximum spreading diameter D_m (Fig. 1). As a result, we can estimate the drop's kinetic energy compared to its surface energy by computing the Weber number $\mathrm{We} = \rho D_0 V^2/\sigma$. In our experiments, We is varied from 0.5 to 500 for water and from 6 to 600 for FC-72.

The test surfaces in most of our experiments are polished silicon plates (silicon wafers, average surface roughness $\approx$ 5 nm). The plate is placed on top of a polished stainless-steel holder (Fig. 1). At the center of the holder, a 2 cm-diameter hole allows for bottom-view observations if a sapphire plate (5 mm) is used instead of the silicon one (0.5 mm). We embed in the holder a temperature probe and six cartridge heaters (Omega, Inc.) symmetrically around the hole to control its temperature and consequently the temperature of the test surface. Since sapphire and silicon both have high thermal conductivity, the temperature difference between the holder and the test surface is only a few degrees and can be neglected in the explored temperature range (from 200 °C to 600 °C). As a result, the surface temperature T is approximated as the holder's temperature.

We repeat the droplet impact experiment numerous times using water as the working fluid for different

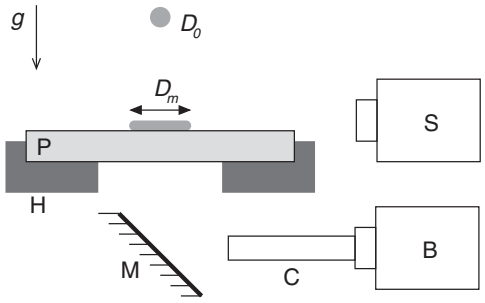

FIG. 1. Schematic of the experimental setup (not drawn to scale) used to study droplet impact on heated surfaces. A liquid droplet of initial diameter $D_0 \approx 2$ mm falls on a heated plate P and spreads to its maximum diameter D_m. The plate P is a polished silicon plate (average roughness ≈ 5 nm) in most experiments. In the case that a bottom view is needed, a polished sapphire plate is used instead of the silicon one. The plate is placed on a holder H which can be heated by six cartridge heaters embedded symmetrically inside. The heaters are monitored by a controller via a solid-state switch (Omega, Inc.). The maximum temperature that can be obtained with this system is 700 °C, with accuracy within 1 K. The holder has a 2 cm-diameter hole in the center allowing bottom-view observation. The side view of the impact is recorded by camera S (Photron SA1), and the bottom view is recorded by camera B (Photron SA2) connected to a long working distance microscope C via a mirror M.

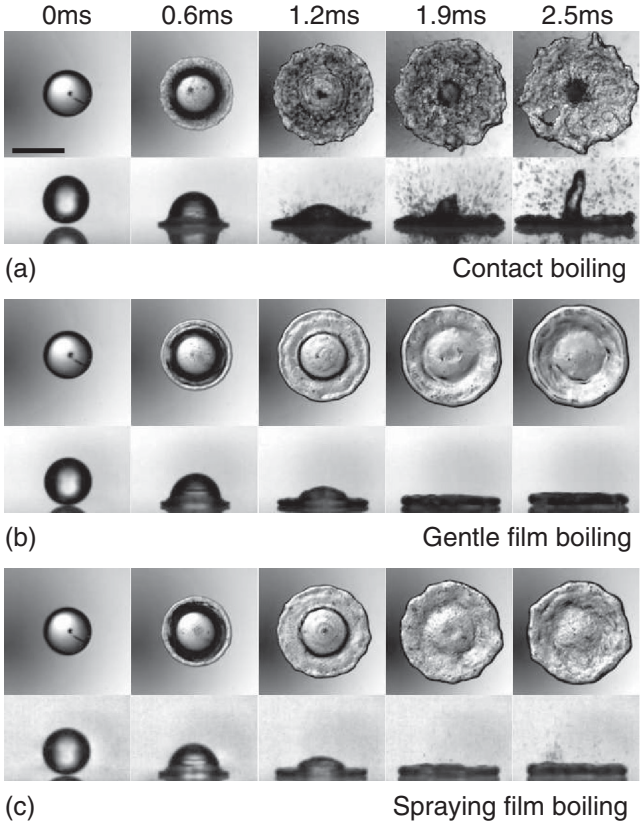

FIG. 2. Series of images of representative water droplet impacts in three regimes. The Weber number in all three experiments is 32. Each image has both bottom view and side view of the impact. Images in the same column are taken at the same time after impact. (a) The surface temperature $T = 380$ °C; contact boiling. The first sign of droplet ejection is seen at 0.6 ms after impact. (b) $T = 500$ °C; gentle film boiling. (c) $T = 580$ °C; spraying film boiling. The contrast of the side-view images was enhanced to show tiny droplets ejected upward at 1.9 ms. The inset bar (shown in upper left image) indicates a length scale of 2.5 mm.

Weber numbers ($0.5 \leq \mathrm{We} \leq 500$) and surface temperatures ($250\,^\circ\mathrm{C} \leq T \leq 560\,^\circ\mathrm{C}$), and observe the drop behavior during impact. Figure 2 shows three distinct impact regimes, each one of which is exemplified by a series of images taken from a high-speed recording of a representative experiment.

Figure 2(a) shows images of an experiment in the contact boiling regime. The bottom views in these images evidently show that shortly after impact, the liquid makes partial contact with the surface. The contact leads to a high rate of heat transfer from the heated surface and consequently formation and growth of vapor bubbles. The vapor pressure increases abruptly causing disruption of the liquid's bottom surface, as well as violent, sometimes explosive, ejection of tiny droplets due to the venting of the vapor bubbles (clearly seen from the side views). In the phase diagram (Fig. 3), this regime corresponds to the region in red color (diamonds).

The gentle film boiling regime is shown in Fig. 2(b). The name refers to situations in which the vapor layer is sufficiently thick to prevent the liquid from touching the surface and there is no droplet ejection due to expansion of vapor bubbles (disintegration of the impacting droplet may happen, but due to other mechanisms, e.g., instability at the rim of the spreading lamella at high Weber number). This regime corresponds to the region in blue color (circles) in Fig. 3.

The spraying film boiling regime [Fig. 2(c)] is similar to the gentle film boiling regime in that the liquid is not in contact with the surface [bottom views in Fig. 2(c)]. However, the side-view images reveal sprayinglike ejection of small droplets from the top of the liquid, although the ejection is not as vigorous as in the case of contact boiling. This regime corresponds to the region in green color (squares) in Fig. 3.

Let us discuss the transition between the contact boiling and the gentle film boiling regimes in Fig. 3. This transition marks the dependence of the dynamic Leidenfrost temperature T_L on the Weber number We. While there have been disparate conclusions regarding whether T_L increases [10,11], or decreases [12,13] with We, our data show unambiguously that T_L increases along with We. We account for this change in T_L by comparing the pressure in the vapor layer and the drop's dynamic pressure: an impinging droplet bounces back from the heated surface (hence in the gentle film boiling regime) if the vapor pressure overcomes the drop's dynamic pressure. Note

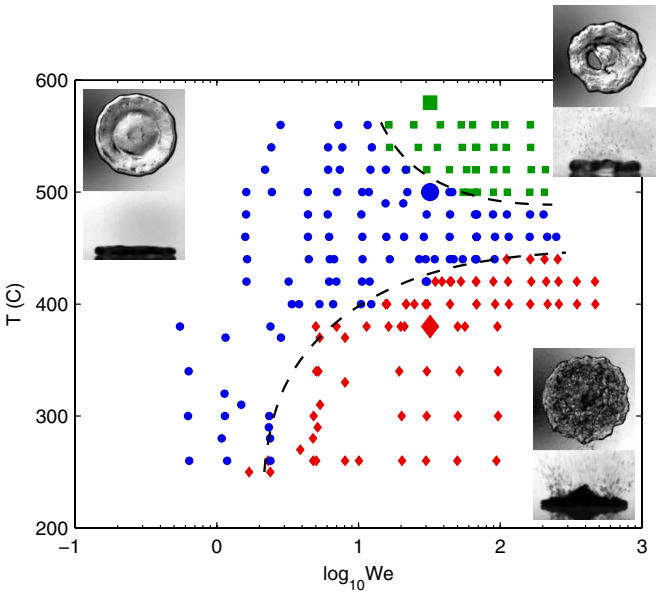

FIG. 3 (color online). Phase diagram for water droplet impact on a heated surface showing three separate regions: contact boiling regime (red solid diamonds), gentle film boiling regime (blue solid circles), spraying film boiling regime (green solid squares). Each region has an inset illustrating the typical droplet impact behavior in that regime. The three large symbols represent the experiments shown in Fig. 2. The dashed lines between different regimes are drawn to guide the eye.

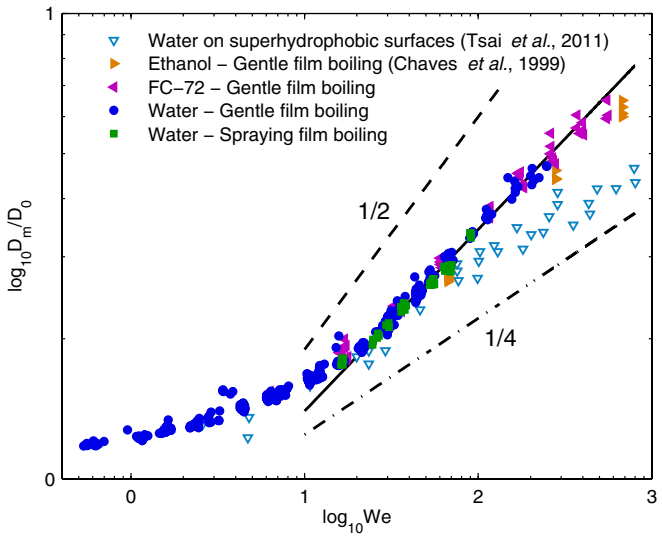

FIG. 4 (color online). Log-log plot of the maximum spreading diameter normalized by the drop's diameter (D_m/D_0) versus the Weber number (We) for impact in both gentle and spraying film boiling regimes. Experimental data for water drops spreading on superhydrophobic surfaces at room temperature by Tsai *et al.* [15] (open downward triangles), ethanol in the gentle film boiling regime by Chaves *et al.* [16] (solid right triangles), FC-72 in the gentle film boiling regime (solid left triangles), water in the gentle film boiling regime (solid circles), water in the spraying boiling regime (solid squares). The Weber number $0.5 \leq \mathrm{We} \leq 600$. The surface temperature $250\,^{\circ}\mathrm{C} \leq T \leq 560\,^{\circ}\mathrm{C}$. The solid line represents the best fit for the experimental data for $\mathrm{We} > 10$ in the present study with the slope 0.39. The dashed line represents the scaling $D_m/D_0 \sim \mathrm{We}^{1/2}$ resulting from the balance between the drop's initial kinetic energy and its surface energy at maximum deformation. The dash-dotted line represents the scaling $D_m/D_0 \sim \mathrm{We}^{1/4}$ resulting from a momentum argument [17].

that increasing the surface temperature raises the vapor pressure and the drop's dynamic pressure is essentially determined by We. Therefore, a higher surface temperature is necessary to keep droplet impact at higher Weber number in the gentle film boiling regime. As a result, we conclude that the dynamic Leidenfrost temperature increases with increasing Weber number, consistent with our experimental results.

The second transition in Fig. 3 is between the gentle and spraying film boiling regimes. From $\mathrm{We} = 11$ and $T = 560\,^{\circ}\mathrm{C}$, the transition temperature decreases with increasing Weber number. To understand this result, we argue that droplet ejection in the spraying film boiling regime is caused by the bursting of vapor bubbles in the liquid film. As We is increased, the liquid film gets thinner and it is easier for the boiling bubbles to burst through the liquid's upper surface. As a result, the transition temperature decreases as the Weber number increases, in accordance with our experimental results. We stress that the bursting of vapor bubbles in the liquid film is a crucial condition for the transition from gentle to spraying film boiling regime. We confirm this by noting that for a fixed Weber number ($\mathrm{We} = 30$), adding 50 μm particles to the liquid (the estimated liquid film thickness is about 300 μm) effectively reduces the transition temperature [14]. This observation implies that the transition from gentle to spraying film boiling regimes is related to the vapor bubble formation inside the liquid film, which is enhanced due to increasing of nucleation sites provided by the particles.

To obtain a quantitative understanding of the spreading dynamics of drop impact on the Leidenfrost vapor layer, we measure the maximum spreading diameter D_m of the drop in the gentle and spraying film boiling regimes and compare it with scaling arguments and experimental data available in the literature [15–17]. In Fig. 4, we show a log-log plot of the dimensionless maximum spreading $\gamma = D_m/D_0$ versus the Weber number. The plot consists of five sets of data: one set was taken using water on superhydrophobic surfaces at room temperature and atmospheric pressure (data by Tsai *et al.* [15]), two sets were taken using water and FC-72 in the gentle film boiling regime, one using water in the spraying boiling regime, one using ethanol in the gentle film boiling regime (data by Chaves *et al.* [16]). Despite a wide variation in surface temperature ($250\,^{\circ}\mathrm{C} \leq T \leq 560\,^{\circ}\mathrm{C}$), and differences in liquid (viscosity, surface tension, density) and thermal properties (heat capacity and latent heat of evaporation) between water, FC-72, and ethanol, all the data in the gentle and spraying film boiling regimes fall on

a unique, single curve, signaling universality of the spreading dynamics in the film boiling regime. For We > 10, our data are best fitted by the scaling $D_m/D_0 \sim \mathrm{We}^{0.39} \approx \mathrm{We}^{2/5}$. This is much steeper than the well-established scaling law $D_m/D_0 \sim \mathrm{We}^{1/4}$ [17] found for the impact of various different liquid droplets on both hydrophilic [17], hydrophobic, and even superhydrophic surfaces (see [15] and the data of that paper which we have included in Fig. 4). In this last situation, the liquid spreading is lubricated by an air layer between the drop and the solid surface. Given the universality of the 1/4-scaling law and the slip due to the air lubrication layer, dissipation clearly does not play a role for the 1/4-scaling law. The steeper and also universal 0.39 scaling is therefore the more remarkable. This effect may be due to an extra driving mechanism caused by the evaporating vapor radially shooting outwards and taking the liquid along. This interpretation is consistent with the experimentally found ambient pressure dependence of D_m/D_0 [15]. Note that balancing the surface energy σD_m^2 and the initial kinetic energy $\rho D_0^3 V^2$ would lead to an even steeper scaling $D_m/D_0 \sim \mathrm{We}^{1/2}$ which is not observed.

While the existence of the vapor layer is crucial in understanding the spreading dynamics and heat transfer of droplet impact on heated surface, there has been hardly any experimental measurement of the thickness of the vapor layer to date. Here, we provide direct measurements of the vapor thickness of drop impact in the gentle film boiling regime using interferometry. In Fig. 5(a), we show the interference pattern from a bottom view of an impinging drop at We $= 3.5$ and $T = 350\,^{\circ}\mathrm{C}$. The novelty here is that by using a color high-speed camera (Photron SA2), we are able to simultaneously obtain interference patterns formed by light of different wavelengths [Fig. 5(a)]. The fringe spacings for different lights are then used to extract the absolute thickness of the vapor [18]. In Fig. 5(b), we show the measured vapor layer profile. Even for the drop at this low Weber number, the vapor thickness is 1 order of magnitude smaller than that in the case of a static Leidenfrost drop at a similar surface temperature (as predicted by Gottfried *et al.* [3] and verified experimentally by Biance *et al.* [19], the vapor thickness is roughly 20 μm in the static case), consistent with our finding that higher velocities require higher surface temperature for the gentle film boiling regime to occur. Surprisingly, the measured vapor thickness is close to the air thickness measured indirectly for drop impacts on unheated surfaces [20].

In conclusion, we have experimentally explored the (We, T) phase space of impact of liquid droplets on heated smooth surfaces. The impact behavior can be separated into three regimes: contact boiling, gentle film boiling, and spraying film boiling. We show that the transition temperature from the contact boiling regime to the gentle film boiling regime (the dynamic Leidenfrost temperature T_L) increases monotonically with increasing Weber number. We also find that the transition temperature from the gentle film boiling to spraying film boiling regime is related to boiling bubbles inside the liquid film and deceases with increasing We. For impacting droplets in both the gentle and the spraying film boiling regimes (both occurring when the surface temperature is higher than T_L), the maximum deformation displays universality regardless of the variation in surface temperature and liquid's properties.

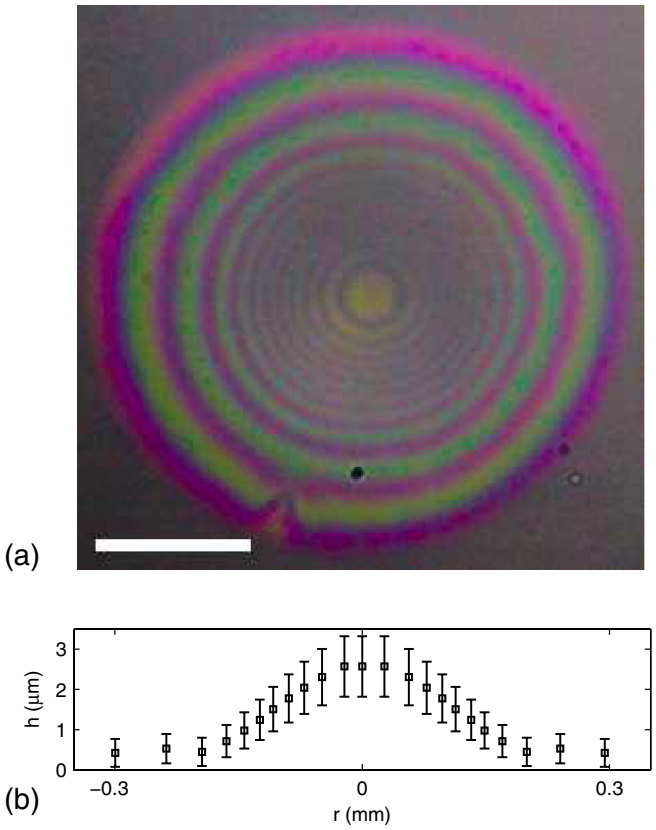

FIG. 5 (color online). (a) Interference pattern showing thickness variation of the vapor layer during impact of a droplet (the image was taken 0.3 ms after the camera detects the droplet). The image was taken from the bottom view of droplet impact using a color high-speed camera connected to a long working distance microscope at 10 000 frames per second. The Weber number is 3.5 and the surface temperature is 350 °C. The inset bar indicates 0.2 mm. (b) Profile of the vapor thickness extracted from the color image.

This study was financially supported by the European Research Council ERC.

*t.tran@utwente.nl
†c.sun@utwente.nl
‡d.lohse@utwente.nl

[1] J. Leidenfrost, Int. J. Heat Mass Transf. **9**, 1153 (1966).
[2] J. Bernardin and I. Mudawar, J. Heat Transfer **121**, 894 (1999).
[3] B. Gottfried, C. Lee, and K. Bell, Int. J. Heat Mass Transf. **9**, 1167 (1966).

[4] J. Bernardin, C. Stebbins, and I. Mudawar, Int. J. Heat Mass Transf. **40**, 247 (1997).
[5] S. Chandra and C. Avedisian, Proc. R. Soc. A **432**, 13 (1991).
[6] K. Anders, N. Roth, and A. Frohn, Exp. Fluids **15**, 91 (1993).
[7] T. Xiong and M. Yuen, Int. J. Heat Mass Transf. **34**, 1881 (1991).
[8] A. Moreira, A. Moita, and M. Panão, Prog. Energy Combust. Sci. **36**, 554 (2010).
[9] M. Rein, *Drop-surface Interactions* (Springer, Wien, New York, 2002), Vol. 456.
[10] S. Yao and K. Cai, Exp. Therm. Fluid. Sci. **1**, 363 (1988).
[11] J. Bernardin and I. Mudawar, J. Heat Transfer **126**, 272 (2004).
[12] A. Wang, C. Lin, and C. Chen, Phys. Fluids **12**, 1622 (2000).
[13] G. Celata, M. Cumo, A. Mariani, and G. Zummo, Heat Mass Transfer **42**, 885 (2006).
[14] A systematic study of the effect of particles on the transition temperature is beyond the scope of this Letter.
[15] P. Tsai, M. Hendrix, R. Dijkstra, L. Shui, and D. Lohse, Soft Matter **7**, 11 325 (2011).
[16] H. Chaves, A. Kubitzek, and F. Obermeier, Int. J. Heat Fluid Flow **20**, 470 (1999).
[17] C. Clanet, C. Béguin, D. Richard, and D. Quéré, J. Fluid Mech. **517**, 199 (2004).
[18] R. van der Veen, T. Tran, D. Lohse, and C. Sun (to be published).
[19] A. Biance, C. Clanet, and D. Quéré, Phys. Fluids **15**, 1632 (2003).
[20] S. T. Thoroddsen *et al.*, J. Fluid Mech. **545**, 203 (2005).